Density Functional Theory Study on the Static Dipole Polarizability of Boron Nitride Nanotubes: Single Wall and Coaxial Systems

ARTICLE *in* THE JOURNAL OF PHYSICAL CHEMISTRY C · JANUARY 2014

Impact Factor: 4.77 · DOI: 10.1021/jp410932a

2 AUTHORS:

Afshan Mohajeri
Shiraz University
68 PUBLICATIONS **556** CITATIONS
SEE PROFILE

Akbar Omidvar
University of Barcelona, Shiraz University
12 PUBLICATIONS **63** CITATIONS
SEE PROFILE

THE JOURNAL OF PHYSICAL CHEMISTRY C

Article

pubs.acs.org/JPCC

Density Functional Theory Study on the Static Dipole Polarizability of Boron Nitride Nanotubes: Single Wall and Coaxial Systems

Afshan Mohajeri* and Akbar Omidvar

Department of Chemistry, College of Sciences, Shiraz University, Shiraz, Iran

ABSTRACT: Optical and electronic properties are evaluated for infinite periodic boron nitride nanotubes (BNNTs) within density functional theory framework. Specifically, the static dipole polarizability and the band gap of the single-walled zigzag and armchair tubes as well as the double-walled zigzag nanotubes are calculated. Four density functional methods of different categories, namely, PBE, TPSS, VSXC, and HSE have been considered for our purpose. Our results allow promising application of the HSE functional in predicting band gap of infinite periodic nanotubes and similar compounds. The behaviors of DFT methods we obtained for single-walled boron nitride nanotubes are also preserved for predicting the band gap and shielding efficiency of double-walled BNNTs. In double-walled coaxial tubes, the interwall interaction is found to reduce the band gap distinctly and to have only minor effects on the polarizabilities of constituent tubes. In contrast with multiwalled carbon nanotubes, where the inner tube is almost completely shielded by the outer tube, in the studied double-walled BNNTs the inner tube is only partially shielded by the outer shell. This study has implication for nanoelectronics and specifically suggests a new route to efficiently design novel nanodevices with tunable gaps.

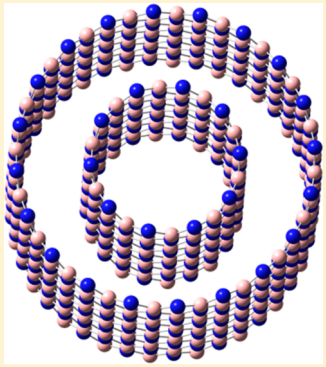

I. INTRODUCTION

Nanotubular materials attract a lot of scientific interest due to their unique properties and great potentials for technological applications. Since the discovery of carbon nanotubes (CNTs),[1] substantial interest has been devoted to predicting the optical response properties of these systems.[2−7] In particular, the prediction and understanding of (hyper) polarizabilities have received attention.[8−13] These studies have interesting implications for nanoelectronics and have been identified as important for a host of potential applications. For example, nanotube polarizability will be important in the emerging uses of nanotubes as electrochemical and field emission devices.[14,15] The polarizability is also critical for understanding the behavior of nanotubes as molecular sensors.[16] For the development of these applications, modeling the response of the nanotubes to a macroscopic electric field or to the field due to nearby molecules is therefore an important issue.

Soon after the discovery of CNTs, it became obvious that similar nanostructures could be formed by other elements and compounds which form layered structures bearing some resemblance to graphite. For example, hexagonal boron nitride (*h*-BN) was predicted on the basis of theoretical calculations[17,18] to be capable of forming nanotubes, a prediction which was later confirmed experimentally by the synthesis of such nanotubes.[19] Although *h*-BN and graphite are isoelectronic, and have very similar structures, the corresponding nanotubes show significant differences in their properties. In particular, boron nitride nanotubes (BNNTs) have a less dramatic dependence of the electrical properties on rolling direction and tube radius.

BNNTs have been the subject of extensive experimental[20−25] and theoretical[26−31] studies due to the unique insulating behavior with ∼5.9 eV band gap regardless of their chirality, tube diameter, and the number of walls.[17] Furthermore, BNNTs exhibit outstanding thermal stability and chemical inertness. The stability of the properties with respect to tube size is an important advantage of BNNTs over CNTs. In particular, as far as the optical and optoelectronic applications of nanotubes are concerned, BNNT could be superior to CNTs. Therefore, the electronic and optical properties of BNNTs are important topics and have been intensively studied theoretically in recent years.

Kongsted et al.[32] investigated the frequency-dependent screened polarizabilities of finitely long single-walled boron nitride nanotubes with a semiempirical dipole−dipole interaction model and ab initio calculations at the SCF level. Their computations showed that BNNTs have smaller magnitude of polarizabilities than those of CNTs with the same geometry and number of atoms. Guo and Lin[33,34] carried out a series of calculations in order to analyze the band structure and linear and nonlinear optical features of several BNNTs using the local density approximation (LDA). They have also applied the finite-field electric-enthalpy theory to study the static dielectric properties of BNNTs.[35] Wang et al.[36] studied static and optical transverse and longitudinal screened polarizabilities of single-walled and multiwalled boron nitride nanotubes by using the density functional perturbation theory (DFPT) within LDA framework. Ab initio finite electric-field calculations were

Received: November 6, 2013
Revised: December 29, 2013
Published: January 13, 2014

Table 1. Mean Polarizability Values per Unit Length (Å^2) and Band Gaps (eV) of the Studied BNNTs

	PBE		VSXC		HSE		TPSS		HF	
	$\bar{\alpha}$	E_g	$\bar{\alpha}$	E_g	$\bar{\alpha}$	E_g	$\bar{\alpha}$	E_g	$\bar{\alpha}$	E_g
(3,0)	8.05	1.23	7.15	1.60	5.71	2.55	7.81	1.35	2.35	8.52
(4,0)	8.73	1.28	7.98	1.66	6.65	2.59	8.34	1.36	2.92	10.33
(5,0)	10.55	1.90	9.83	2.17	8.13	3.19	10.08	2.02	3.64	10.80
(6,0)	12.46	2.64	11.67	2.87	9.67	3.96	11.91	2.78	4.36	11.58
(7,0)	14.36	3.30	13.18	3.65	11.18	4.65	13.74	3.45	5.05	12.34
(8,0)	16.27	3.47	14.93	3.84	12.71	4.82	15.58	3.62	5.75	12.54
(9,0)	18.20	3.72	16.70	4.09	14.23	5.08	17.43	3.88	6.45	12.84
(10,0)	20.12	3.99	18.47	4.36	15.76	5.36	19.28	4.15	7.21	13.04
(11,0)	21.77	4.07	20.0	4.46	17.12	5.45	20.87	4.24	7.90	13.13
(3,3)	10.23	4.30	9.60	4.55	8.07	5.79	9.82	4.49	3.85	13.69
(4,4)	13.66	4.29	12.61	4.76	10.77	5.73	13.09	4.47	5.04	13.61
(5,5)	17.46	4.24	16.03	4.66	13.65	5.65	16.72	4.42	6.34	13.30
(6,6)	21.18	4.41	19.43	4.84	16.56	5.84	20.29	4.60	7.51	13.61
(7,7)	24.27	4.50	22.28	4.94	19.04	5.93	23.27	4.68	8.67	13.73
(8,8)	27.63	4.52	25.36	4.96	21.69	5.95	26.49	4.71	9.89	13.79
(9,9)	30.72	4.63	28.26	5.06	24.22	6.06	29.52	4.81	11.23	13.78
(10,10)	34.15	4.62	31.41	5.05	26.92	6.05	32.81	4.80	12.46	13.78
(11,11)	38.45	4.46	35.68	4.84	30.13	5.87	36.87	4.64	13.71	13.64
(3,0)@(9,0)	31.35	0.69	27.14	1.03	22.66	1.80	30.05	0.77		
(3,0)@(10,0)	30.10	0.92	27.11	1.05	22.56	1.98	29.02	1.01		
(3,0)@(11,0)	31.18	0.46	28.89	0.59	23.49	1.51	29.95	0.50		

performed by Lan and co-workers[37] to study the static transverse dielectric properties of BNNTs via the sawtooth potential approach. The most recent treatment of the linear and nonlinear electric dipole susceptibilities of infinite periodic zigzag BNNTs has been carried out by the coupled perturbed Kohn−Sham scheme.[38−40]

However, despite extensive theoretical studies, only a few density functional theory (DFT) calculations of the optical properties of BNNTs have been reported. Due to its favorable scaling with system size and reasonable accuracy in many applications, DFT has been regarded as one of the most powerful theoretical tools for studying both electronic and dynamic properties of medium to large ground state systems. On the other hand, in view of the well-known overshoot of polarizabilities obtained for LDA in quasi-1D systems,[41−43] a comparison with other density functionals and, particularly, with the hybrid functionals is of interest. Accordingly, to broaden the search space and enrich the available information of theoretical studies, as the main objective of the present work we report a DFT calculation on the both transverse and longitudinal polarizabilities of single-walled and coaxial double-walled BNNTs. Indeed our emphasis is on the trends in the data as they are obtained from DFT calculations by employing different exchange-correlation functionals, to create empirical rules for polarizability of BNNTs.

Herein, we draw our attention to the small-diameter BNNTs. In fact, when the diameter of BNNT is less than 9.5 Å the band gap would decrease rapidly with decreasing diameter due to the curvature effect as shown in previous calculations.[44,45] This inspires us that when the BNNT enters into small size, a semiconductor with changeable band gap should be suitable for applications in nanoelectronics and photonic devices. On the other hand, due to the ionicity of B−N bonds, the wall buckling can greatly lower the energies of small BNNTs and enhance their stability with respect to the CNTs with similar diameter.[46] From these viewpoints, the study on the polarizability of small BNNTs should be more interesting than those performed for CNT counterparts.

The rest of this paper is organized as follows. In section II, the theoretical approach and computational details are briefly described. Our results are reported and discussed in section III. Aspects covered include static polarizability and band gap of single-walled BNNTs utilizing DFT methods, the effect of exact exchange on the computed properties, the dependence of longitudinal and transverse polarizabilities on the tube diameter and on the band gap, and the effect of interwall interaction on the optical properties of double-walled BNNTs. Finally, in section IV, a summary is given.

II. COMPUTATIONAL DETAILS

All calculations reported in this study were carried out using the GAUSSIAN09 suite of programs[47] with periodic boundary conditions (PBC). Both zigzag (n,0) and armchair (n,n) nanotubes with n ranging from 3 to 11 were examined. The unit cell under consideration contained 4n atoms regardless of the tube type. All nanotube geometries were generated by TubeGen[48] and used after optimization. Four density functional methods belonging to different categories of DFT methods have been tested. In particular, one functional of generalized gradient approximation (GGA) type, PBE,[49] two meta-GGA functionals. VSXC[50] and TPSS,[51] and one hybrid-GGA functional, HSE,[52] have been assessed.

One potential criticism of using DFT for polarizabilities is the well-known overestimation of this property in extended systems by most commonly used density functionals.[53] It has been argued that exact exchange makes the calculation of polarizability more accurate.[54] Therefore it was deemed necessary to perform some calculations with exact exchange in this study. Accordingly, we have included Hartree−Fock (HF) method and also the functional HSE which contains exact exchange in its short-range of the Coulomb potential.

All geometry optimizations and polarizability calculations were performed by use of 6-31+G(d) basis set with 40 **k** points.

dx.doi.org/10.1021/jp410932a | J. Phys. Chem. C 2014, 118, 1739−1745

The selection of suitable basis set is an important task which should be carried out with care in order to advance safely to prediction of reliable properties. In the context of basis sets assessment and construction of large, flexible, and adequately polarized basis in electronic property and dipole polarizability calculations, many efforts have been carried out in the literature.[55−57] The 6-31+G(d) basis set was chosen as a compromise between speed and accuracy. Larger basis set can change the quantitative value of the calculated polarizabilities but do not change the trends in the data. Moreover, the sufficiency of this basis set for determination of total energy, band gap, and polarizability has been demonstrated recently.[38]

For calculation of the polarizability components tensor, we relied on the finite field (FF) approach.[58,59] A field strength of 0.001 au (equivalent to 0.03 eV) along the transverse direction was used. The polarizabilities were initially computed per unit cell and then converted to a polarizability per angstrom of length, easing comparison between the armchair and zigzag tubes.

III. RESULTS AND DISCUSSION

A. Single-Walled BNNT (SWBNNT). The computed mean polarizabilities [$\bar{\alpha} = (1/3)(2\alpha_{\perp} + \alpha_{\parallel})$] and the energy gap ($E_g$) between highest occupied crystalline orbital (HOCO) and lowest unoccupied crystalline orbital (LUCO) for all nanotubes examined in this study are collected in Table 1. Despite the differences observed in the method performance, the values listed in Table 1 indicate that the main trend that is observed at HF level holds for all DFT methods we tested. However, the HF provides lower polarizabilities compared to the DFT results by approximately 60−70% for PBE, TPSS, and VSXC functionals and about 50−60% for HSE method. The tendency of DFT methods to overestimate polarizabilities is related to the incorrect asymptotic decay of the exchange-correlation potential. Among DFT methods we tested, pure functionals including PBE, TPSS, and VSXC yield very similar results whereas the HSE method as hybrid functional provides much lower polarizability values. However, the change in polarizability with the size of nanotube is similar for all tested functionals.

Now, we discuss the method performance in predicting the polarizability components and also band gaps of studied BNNTs. Figure 1 presents the longitudinal ($\alpha_{\parallel}$) and transverse ($\alpha_{\perp}$) polarizabilities per unit length of BNNTs versus their diameter. For all examined DFT methods both the longitudinal and transverse components vary linearly with the tube diameter. However, a recent work of Orlando et al.[39] shows curvature for the polarizability components at the larger values of diameter indicating different behaviors for BNNTs with small and large diameters.

Unfortunately, due to difficulties in the purification of synthesized SWBNNT samples,[60] no experimental measurements of the optical properties are available. However, it is well-known that the polarizabilities are strongly influenced by the band gap. Experimental band gap of 5.8−5.9 eV has been reported by Arenal et al.[61] for SWBNNTs and by Jaffrennou et al.[22] and Lee et al.[62] for multiwalled BNNTs. The calculated band gap for the (11,0) nanotube considered here is between 4.07 and 4.46 eV with PBE, VSXC, and TPSS functionals, whereas it is much larger (13.13 eV) in the HF approximation. Thus we observed an underestimation of band gap with GGA forms of DFT and overestimation by HF method. To solve the band gap problem, an alternative approach is the hybrid

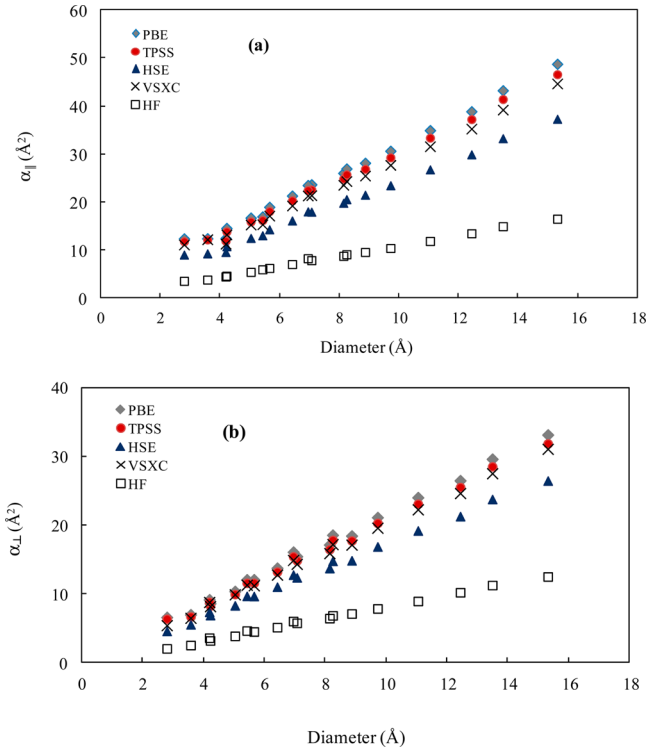

Figure 1. Comparison of DFT and HF methods. Longitudinal $\alpha_{\parallel}$ (a) and transverse $\alpha_{\perp}$ (b) polarizabilities per unit length of SWBNNTs versus the tube diameter.

functional schemes which include a fraction of HF exact exchange in the purely density-dependent exchange-correlation functionals. This leads to some combining the overestimation of band gaps from HF with the underestimation from GGA and would improve the predicted band gaps.

The considered hybrid functional in this study is HSE which derives from the PBE0[63] and includes 25% exact HF exchange. The HSE method has been validated for the band gap calculations of semiconductors and produces errors over five times smaller than pure DFT results.[64] Moreover, HSE has been successfully applied for periodic boundary calculations to predict lattice constant and bulk moduli of metals, semiconductors, and insulators.[65] However, in agreement with prior calculations, the superior performance of HSE functional has also been demonstrated for studied BNNTs in the present study. The band gap of (11,0) tube we obtained with HSE method is 5.45 eV, which is in good agreement with experimental value (5.8−5.9 eV). Even considering that real samples contain much larger radius nanotubes than the (11,0) case and that the band gap calculated with HSE reaches about 5.9 eV for very large SWBNNTs, we conclude that the hybrid functionals, particularly the HSE method, perform the best as far as optical properties are concerned.

Like CNTs,[6] the static polarizability of BNNTs is found to scale with R/E_g^2, where R is the radius. In Figure 2, we observe that the polarizabilities per unit length of armchair BNNTs have linear relation with R/E_g^2 while those of zigzag structures do not present such dependency. The band gaps in armchair SWBNNTs are approximately constant; hence, $\bar{\alpha} \sim R/E_g^2$ and $\bar{\alpha} \sim R$ are actually equivalent. However, for zigzag SWBNNTs the applicability of $\bar{\alpha} \sim R/E_g^2$ may be possible for large radius tubes in which the variation of band gap becomes negligible.

dx.doi.org/10.1021/jp410932a | J. Phys. Chem. C 2014, 118, 1739−1745

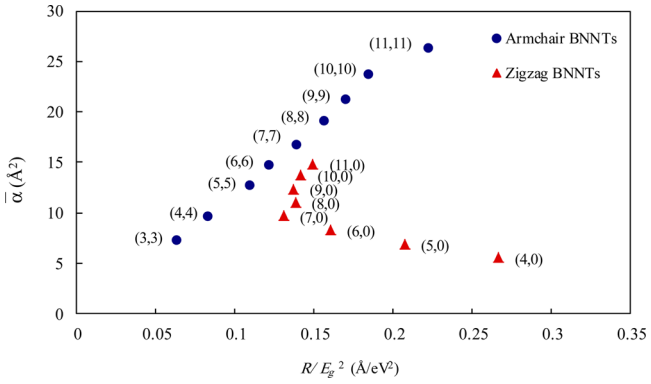

Figure 2. Mean polarizability per unit length of SWBNNTs calculated with the HSE method as a function of R/E_g^2, where R is the radius and E_g is the band gap.

Finally, we close our discussion on the SWBNNTs by emphasizing the role of tube geometry on the calculated polarizability. In Table 2, the polarizability of an armchair and a zigzag conformation, both with 44 boron and nitrogen atoms, are compared. For both structures, the polarizability along the tube is higher than the transverse component implying that under the influence of an external electric field, the electronic density along the direction of the tube were more easily polarized with respect to the perpendicular direction. For the armchair tube, the polarizability components, mean polarizability, and anisotropy of the polarizability are larger than the corresponding values in the zigzag configuration. This trend has also been reported for the polarizability[66,67] and for the mean static hyperpolarizability[68,69] of CNTs. From the results of Table 2 it is observed that despite significant difference between the optical properties of armchair and zigzag structures, the calculated band gaps of mentioned tubes are almost the same.

Table 2. Comparison of the Structural Parameters and Optical and Electronic Properties between Zigzag and Armchair BNNT: Tube Diameter (D)[a], Length of Translational Vector (T), Transverse ($\alpha_\perp$), Longitudinal ($\alpha_\parallel$), and Mean ($\bar{\alpha}$) Polarizabilities per Unit Length, Anisotropy of the Polarizability ($\Delta\alpha$),[b] and Band Gap (E_g).[c]

	D (Å)	T (Å)	$\alpha_\perp$ (Å²)	$\alpha_\parallel$ (Å³)	$\bar{\alpha}$ (Å²)	$\Delta\alpha$ (Å²)	E_g (eV)
(11,0)	8.91	4.36	14.85	21.44	17.12	5.38	5.45
(11,11)	14.94	2.51	26.45	37.29	30.13	8.85	5.87

[a]In zigzag structure the tube diameter is the distance between two opposite nitrogen atoms, and in armchair tube the diameter is the distance between opposite boron and nitrogen atoms. [b]Mean polarizability $\bar{\alpha} = (1/3)(2\alpha_\perp + \alpha_\parallel)$. Anisotropy of the polarizability $\Delta\alpha = [2(\alpha_\perp - \bar{\alpha})^2 + (\alpha_\parallel - \bar{\alpha})^2]^{1/2}$. [c]The reported data were calculated at the HSE/6-31+G(d) level of theory.

B. Double-Walled BNNT (DWBNNT). We have so far focused only on the optical properties of SWBNNTs. However, BNNTs are usually multiwalled. Therefore, to study the possible effects of interwall interactions on the optical properties of BNNTs, we have also calculated the static polarizability and band gaps of four double-walled BNNTs, namely, the (3,0)@(8,0), (3,0)@(9,0), (3,0)@(10,0), and (3,0)@(11,0). These DWBNNTs are chosen because the experimental electron diffraction analysis has revealed that BNNTs typically possess zigzag atomic arrangement.[70]

First, we discuss the energetics of DWBNNTs with respect to interwall spacing. The interaction energies which are calculated as the energy difference between the total energy of the combined system and the summation of the total energies of two freestanding component nanotubes are shown in Figure 3. The computed interaction energies reveal that the

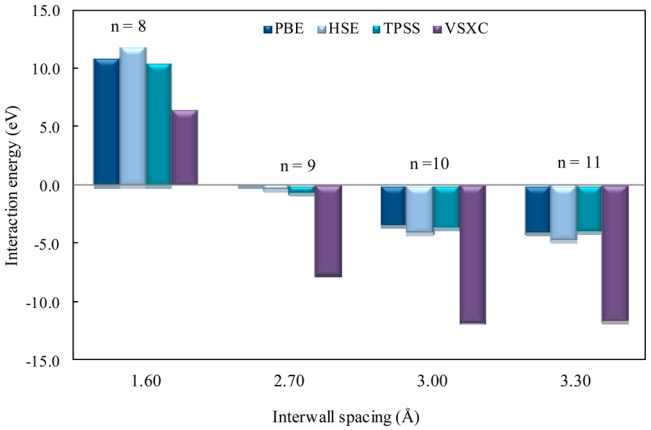

Figure 3. Interaction energy of (3,0)@(n,0) DWBNNTs versus the interwall spacing calculated with studied DFT methods.

double-walled (3,0)@(8,0) is energetically unstable. The optimal pair with the largest negative value of interaction energy is (3,0)@(11,0), which has an interwall spacing of 3.3 Å that is close to interlayer distance in h-BN. This finding is consistent with prior LDA calculation which indicates the configurations for $n \geq 3$ comply with the optimum rule of (n,0)@(n + 8,0) in normal-sized DWBNNTs.[71]

Regarding the method performance, it turned out that PBE, HSE, and TPSS functionals behave quite similarly in predicting the interaction energies while the VSXC method provides different results. For instance, the calculated interaction energy for (3,0)@(11,0) is about −4.0 eV for PBE, HSE, and TPSS methods, whereas it is −11.7 eV with VSXC functional.

Now, after discussing the stability of coaxial BNNTs, we particularly clarify the static polarizability of (3,0) BNNT encapsulated in the outer (n,0) shell. Excluding the unstable (3,0)@(8,0) system, the results are presented for n = 9−11. Also, due to low stability of the (3,0)@(9,0) system, some unusual behavior may be observed in the reported data. However, as shown in Figure 4, the longitudinal components of polarizabilities of these DWBNNTs are approximately the sum

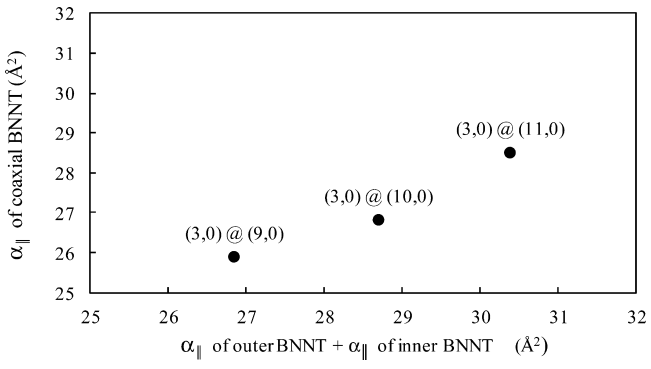

Figure 4. Longitudinal polarizabilities per unit length of coaxial DWBNNTs calculated with the HSE method.

dx.doi.org/10.1021/jp410932a | J. Phys. Chem. C 2014, 118, 1739−1745

of the longitudinal polarizabilities of the constituent tubes, which in turn indicates that the depolarization effects along the tube axis are negligible and the dielectric interaction along the tube axis between constituent tubes is quite weak. The additive property of the longitudinal response has also been shown for multiwalled CNTs.[6] Alternatively, it has been demonstrated that the transverse polarizability of coaxial CNTs is almost the same as the polarizability of the outer nanotube alone.[72] This shielding effect comes from the lack of polarization in the inner tube. However, our results for the examined DWBNNTs indicate that the largest contributions to the transverse polarizabilities come from the outer tube and the role of the inner (3,0) tube is less. Quantitative demonstration of shielding can be found in Figure 5, which represents the difference

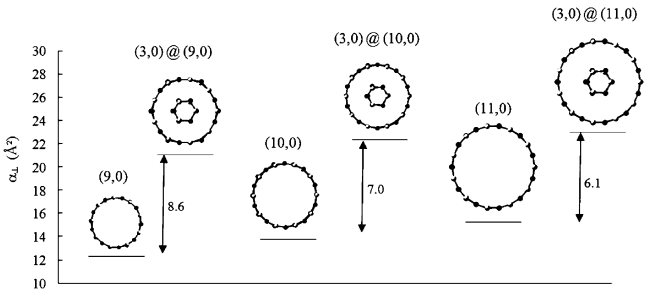

Figure 5. Comparison of the transverse polarizabilities per unit length in coaxial DWBNNTs and their corresponding outer tube calculated at the HSE level.

between transverse polarizability of DWBNNTs and their corresponding outer shells. Inspection of this figure reveals that complete shielding of the inner tube by the outer shell does not occur for the studied DWBNNTs. The shielding efficiency of the outer tube increases as the interwall spacing increases. However, the nearly complete shielding effects in multiwalled CNTs are attributed to their delocalized π-electrons. On the contrary, BNNTs as macroscopic insulating tubes with localized valence electrons hardly produce shielding effects.

It has been shown that the energy gap of a DWBNNT is distinctly reduced from that of the freestanding inner tube.[73] Apparently, the gap reduction is induced by a misalignment between the energy gaps of the inner and outer BNNTs due to hybridization between σ and π states. The calculated band gaps of (3,0)@(10,0) and (3,0)@(11,0) tubes are, respectively, 0.92 (1.98) and 0.46 (1.51) eV at PBE (HSE) level(s) indicating significant reduction from that of the freestanding (3,0) tube. Furthermore, it is found that the decrease in band gap becomes more as the interwall spacing increases; i.e., among the studied DWBNNTs the smallest band gap belongs to the (3,0)@(11,0). The smaller band gap of DWBNNTs and sensitive dependence of the band gap on interwall spacing suggests a new route to efficiently design novel nanodevices with tunable gaps for electronic and optical applications. Finally, it is interesting to note that the behavior of DFT methods we obtained for SWBNNTs also holds for the DWBNNTs. Again, the performances of PBE, TPSS, and VSXC functionals are similar in predicting the band gap and shielding efficiency of DWBNNTs, while the result of HSE is quite different.

IV. CONCLUSIONS

In this article, we compared the performance of DFT methods in determination of linear response of isolated infinite periodic SWBNNTs as well as DWBNNTs to electric-field perturbation. Four functionals belonging to families GGA, meta-GGA, and hybrid-GGA have been considered for our purpose. The behavior of the examined functionals has been assessed for prediction of static dipole polarizabilities and band gaps of $(n,0)$ and (n,n) nanotubes with n = 3−11. It is seen that the values determined by pure GGA functionals (PBE, TPSS, and VSXC) are very different from those obtained by HSE as a hybrid functional. However, the change in polarizability with size of nanotube is similar for all studied functionals. In comparing the calculated band gaps with the experimental value, a convincing performance for HSE functional has been observed. The superiority of HSE method can be attributed to the inclusion of exact exchange in its short-range of the Coulomb potential.

The stability and optical properties of DWBNNTs have also been studied in the framework of DFT. In contrast with multiwalled carbon nanotubes, where the inner tube is almost completely shielded by the outer tube, in the studied DWBNNTs the inner tube is only partially shielded by the outer tube.

All these findings on the small BNNTs provide new features of BN materials for electronic and optical applications. The results presented here show that there are currently several competitive alternatives of DFT methods for determination of electronic and optical properties of periodic systems and still there is no universal best behavior functional. However, further insight into the nature of functionals targeted toward the development of new density functionals for calculating the optical properties of infinite periodic nanotubes and similar compounds is necessary.

AUTHOR INFORMATION

Corresponding Author

*E-mail: amohajeri@shirazu.ac.ir. Phone: +98-7116137161. Fax: +98-7116460788.

Notes

The authors declare no competing financial interest.

ACKNOWLEDGMENTS

Shiraz University is gratefully acknowledged for generous allocation of computational resources and financial support.

REFERENCES

(1) Iijima, S. Helical Microtubules of Graphitic Carbon. *Nature* **1991**, *354*, 56−58.

(2) Liu, X.; Si, J.; Chang, B.; Xu, G.; Yang, Q.; Pan, Z.; Xi, S.; Ye, P. Third-Order Optical Nonlinearity of the Carbon Nanotubes. *Appl. Phys. Lett.* **1999**, *74*, 164−164−6.

(3) Jensen, L.; Schmidt, O. H.; Mikkelsen, K. V.; Åstrand, P.-O. Static and Frequency-Dependent Polarizability Tensors for Carbon Nanotubes. *J. Phys. Chem. B* **2000**, *104*, 10462−10466.

(4) Lü, W.; Dong, J.; Li, Z.-Y. Optical Properties of Aligned Carbon Nanotube Systems Studied by the Effective-Medium Approximation Method. *Phys. Rev. B* **2000**, *63*, 033401−033401−4.

(5) Wang, S.; Huang, W.; Yang, H.; Gong, Q.; Shi, Z.; Zhou, X.; Qiang, D.; Gu, Z. Large and Ultrafast Third-Order Optical Non-Linearity of Single-Wall Carbon Nanotubes at 820 nm. *Chem. Phys. Lett.* **2000**, *320*, 411−414.

(6) Kozinsky, B.; Marzar, N. Static Dielectric Properties of Carbon Nanotubes from First Principles. *Phys. Rev. Lett.* **2006**, *96*, 166801−166801−4.

(7) Sun, S. L.; Hu, Y. Y.; Xu, H. L.; Su, Z. M.; Hao, L. Z. Probing the Linear and Nonlinear Optical Properties of Nitrogen-Substituted Carbon Nanotube. *J. Mol. Model.* **2012**, *18*, 3219−3225.

(8) Jensen, L.; Åstrand, P. O.; Mikkelsen, K. V. Saturation of the Third-Order Polarizability of Carbon Nanotubes Characterized by a Dipole Interaction Model. *Nano Lett.* **2003**, *3*, 661−665.
(9) Guo, G. Y.; Chu, K. C.; Wang, D-s.; Duan, C.-g. Static Polarizability of Carbon Nanotubes: Ab Initio Independent-Particle Calculations. *Comput. Mater. Sci.* **2004**, *30*, 269−273.
(10) Brothers, E. N.; Kudin, K. N.; Scuseria, G. E. Transverse Polarizabilities of Carbon Nanotubes: A Hartree-Fock and Density Functional Study. *Phys. Rev. B* **2005**, *72*, 033402−033402−5.
(11) Brothers, E. N.; Scuseria, G. E.; Kudin, K. N. Longitudinal Polarizability of Carbon Nanotubes. *J. Phys. Chem. B* **2006**, *110*, 12860−12860−4.
(12) Brothers, E. N.; Izmaylov, A. F.; Scuseria, G. E.; Kudin, K. N. Analytically Calculated Polarizability of Carbon Nanotubes: Single Wall, Coaxial, and Bundled Systems. *J. Phys. Chem. C* **2008**, *112*, 1396−1400.
(13) Chai, G. L.; Lin, C. S.; Wei, J.; Zhang, M. Y.; Cheng, W. D. Nonlinear Optical Properties of Carbon Nitride Nanotubes. *Phys. Chem. Chem. Phys.* **2012**, *14*, 835−839.
(14) Baughman, R. H.; Zakhidov, A. A.; de Heer, W. A. Carbon Nanotubes: The Route Toward Applications. *Science* **2002**, *297*, 787−792.
(15) Zhang, M.; Fang, S.; Zakhidov, A. A.; Lee, S. B.; Aliev, A. E.; Williams, C. D.; Atkinson, K. R.; Baughman, R. H. Strong, Transparent, Multifunctional, Carbon Nanotube Sheets. *Science* **2005**, *309*, 1215−1219.
(16) Arab, M.; Picaud, F.; Devel, M.; Ramseyer, C.; Girardet, C. Molecular Selectivity Due to Adsorption Properties in Nanotubes. *Phys. Rev. B: Condens. Matter Mater. Phys.* **2004**, *69*, 165401−165401−11.
(17) Rubio, A.; Corkill, J. L.; Cohen, M. L. Theory Of Graphitic Boron Nitride Nanotubes. *Phys. Rev. B* **1994**, *49*, 5081−5081−4.
(18) Blase, X.; Rubio, A.; Louie, S. G.; Cohen, M. L. Stability and Band Gap Constancy of Boron Nitride Nanotubes. *Europhys. Lett.* **1994**, *28*, 335−340.
(19) Chopra, N. G.; Luyken, R. J.; Cherrey, K.; Crespi, V. H.; Cohen, M. L.; Louie, S. G.; Zettl, A. Boron Nitride Nanotubes. *Science* **1995**, *269*, 966−967.
(20) Grujicica, M.; Cao, G.; Roy, W. N. Suitability of Boron-Nitride Single-Walled Nanotubes as Fluid-Flow Conduits in Nano-Valve Applications. *Appl. Surf. Sci.* **2005**, *246*, 149−158.
(21) Arenal, R.; Stéphan, O.; Kociak, M.; Taverna, D.; Loiseau, A.; Colliex, C. Electron Energy Loss Spectroscopy Measurement of the Optical Gaps on Individual Boron Nitride Single-Walled and Multiwalled Nanotubes. *Phys. Rev. Lett.* **2005**, *95*, 127601−127601−4.
(22) Jaffrennou, P.; Donatini, F.; Barjon, J.; Lauret, J. S.; Maguer, A.; Attal-Trétout, B.; Ducastelle, F.; Loiseau, A. Cathodoluminescence Imaging and Spectroscopy on a Single Multiwall Boron Nitride Nanotube. *Chem. Phys. Lett.* **2007**, *442*, 372−375.
(23) Jaffrennou, P.; Barjon, J.; Lauret, J. S.; Maguer, A.; Golberg, D.; Attal-Trétout, B.; Ducastelle, F.; Loiseau, A. Optical Properties of Multiwall Boron Nitride Nanotubes. *Phys. Status Solidi B* **2007**, *244*, 4147−4151.
(24) Lee, C. H.; Wang, J.; Kayatsha, V. K.; Huang, J. Y.; Yap, Y. K. Effective Growth of Boron Nitride Nanotubes by Thermal Chemical Vapor Deposition. *Nanotechnology* **2008**, *19*, 455605−455605−5.
(25) Lee, C. H.; Xie, M.; Kayashta, V.; Wang, J.; Yap, Y. K. Patterned Growth of Boron Nitride Nanotubes by Catalytic Chemical Vapor Deposition. *Chem. Mater.* **2010**, *22*, 1782−1787.
(26) Sun, C.; Yu, H.; Xu, L.; Ma, Q.; Qian, Y. Recent Development of the Synthesis and Engineering Applications of One-Dimensional Boron Nitride Nanomaterials. *J. Nanomater.* **2010**, *2010*, 163561−1635616.
(27) Guo, G. Y.; Lin, J. C. Systematic Ab Initio Study of the Optical Properties of BN Nanotubes. *Phys. Rev. B* **2005**, *71*, 165402−1654012−3.
(28) Hao, S.; Zhou, G.; Duan, W.; Wu, J.; Gu, B. L. Tremendous Spin-Splitting Effects in Open Boron Nitride Nanotubes: Application to Nanoscale Spintronic Devices. *J. Am. Chem. Soc.* **2006**, *128*, 8453−8458.
(29) Guo, G. Y.; Ishibashi, S.; Tamura, T.; Terakura, K. Static Dielectric Response and Born Effective Charge of BN Nanotubes from ab Initio Finite Electric Field Calculations. *Phys. Rev. B* **2007**, *75*, 245403−245403−9.
(30) Benedict, L. X.; Louie, S. G.; Cohen, M. L. Static Polarizabilities of Single-Wall Carbon Nanotubes. *Phys. Rev. B* **1995**, *52*, 8541−8541−9.
(31) Margulis, V. A.; Muryumin, E. E.; Gaiduk, E. A. Second-Order Nonlinear Optical Response of Zigzag BN Single-Walled Nanotubes. *Phys. Rev. B* **2010**, *82*, 235426−235426−43.
(32) Kongsted, J.; Osted, A.; Jensen, L.; Åstrand, P. O.; Mikkelsen, K. V. Frequency-Dependent Polarizability of Boron Nitride Nanotubes: A Theoretical Study. *J. Phys. Chem. B.* **2001**, *105*, 10243−10248.
(33) Guo, G. Y.; Lin, J. C. Systematic ab Initio Study of the Optical Properties of BN Nanotubes. *Phys. Rev. B* **2005**, *71*, 165402−165402−13.
(34) Guo, G. Y.; Lin, J. C. Second-Harmonic Generation and Linear Electro-Optical Coefficients of BN Nanotubes. *Phys. Rev. B* **2005**, *72*, 075416−0754116−29.
(35) Guo, G. Y.; Ishibashi, S.; Tamura, T.; Terakura, K. Static Dielectric Response and Born Effective Charge of BN Nanotubes from Ab Initio Finite Electric Field Calculations. *Phys. Rev. B* **2007**, *75*, 245403−245403−9.
(36) Wang, L.; Lu, J.; Lai, L.; Song, W.; Ni, M.; Gao, Z.; Mei, W. N. Static and Optical Transverse and Longitudinal Screened Polarizabilities of Boron Nitride Nanotubes. *J. Phys. Chem. C* **2007**, *111*, 3285−3289.
(37) Lan, H. P.; Ye, L. H.; Zhang, S.; Peng, L. M. Transverse Dielectric Properties of Boron Nitride Nanotubes by ab Initio Electric Field Calculations. *Appl. Phys. Lett.* **2009**, *94*, 183110−183110−3.
(38) Ferrabone, M.; Kirtman, B.; Rérat, M.; Orlando, R.; Dovesi, R. Polarizability and Hyperpolarizability of BN Zigzag Nanotubes Calculated by the Coupled Perturbed Kohn−Sham Scheme. *Phys. Rev. B* **2011**, *83*, 235421−235421−9.
(39) Orlando, R.; Bast, R.; Ruud, K.; Ekström, U.; Ferrabone, M.; Kirtman, B.; Dovesi, R. The First and Second Static Electronic Hyperpolarizabilities of Zigzag Boron Nitride Nanotubes. An ab Initio Approach through the Coupled Perturbed Kohn−Sham Scheme. *J. Phys. Chem. A* **2011**, *115*, 12631−12637.
(40) Ferrabone, M.; Kirtman, B.; Lacivita, V.; Rérat, M.; Orlando, R.; Dovesi, R. Vibrational Contribution to Static and Dynamic (Hyper) Polarizabilities of Zigzag BN Nanotubes Calculated by the Finite Field Nuclear Relaxation Method. *Int. J. Quantum Chem.* **2012**, *112*, 2160−2170.
(41) Gisbergen, V. S. J. A.; Schipper, P. R. T.; Gritsenko, O. V.; Baerends, E. J.; Snijders, J. G.; Champagne, B.; Kirtman, B. Electric Field Dependence of the Exchange-Correlation Potential in Molecular Chains. *Phys. Rev. Lett.* **1999**, *83*, 694−694−7.
(42) Loboda, O.; Zalesny, R.; Avramopoulos, A.; Luis, J. M.; Kirtman, B.; Tagmatarchis, N.; Reis, H.; Papadopoulos, M. G. Linear and Nonlinear Optical Properties of [60] Fullerene Derivatives. *J. Phys. Chem. A* **2008**, *113*, 1159−1170.
(43) Kummel, S.; Kronik, L.; Perdew, J. P. Electrical Response of Molecular Chains from Density Functional Theory. *Phys. Rev. Lett.* **2004**, *93*, 213002−213002−5.
(44) Xiang, H. J.; Yang, J.; Hou, J. G.; Zhu, Q. First-Principles Study of Small-Radius Single-Walled BN Nanotubes. *Phys. Rev. B* **2003**, *68*, 035427−035427−31.
(45) Wirtz, L.; Marini, A.; Rubio, A. Excitons in Boron Nitride Nanotubes: Dimensionality Effects. *Phys. Rev. Lett.* **2006**, *96*, 126104−126104−7.
(46) Zhang, Z.; Guo, W.; Dai, Y. Stability and Electronic Properties of Small Boron Nitride Nanotubes. *J. Appl. Phys.* **2009**, *105*, 084312−084312−8.
(47) Frisch, M. J.; et al. *Gaussian 09*, revision A.02; Gaussian, Inc.: Wallingford, CT, 2009.

(48) Frey, J. T.; Doren, D. J. TubeGen 3.4; University of Delaware, Newark, DE, 2011.
(49) Perdew, J. P.; Burke, K.; Ernzerhof, M. Generalized Gradient Approximation Made Simple. *Phys. Rev. Lett.* **1996**, *77*, 3865−3865−8.
(50) Voorhis, T. V.; Scuseria, G. E. A Novel Form for the Exchange-Correlation Energy Functional. *J. Chem. Phys.* **1998**, *109*, 400−400−11.
(51) Tao, J.; Perdew, J. P.; Staroverov, V. N.; Scuseria, G. E. Climbing the Density Functional Ladder: Nonempirical Meta-Generalized Gradient Approximation Designed for Molecules and Solids. *Phys. Rev. Lett.* **2003**, *91*, 146401−146401−4.
(52) Heyd, J.; Scuseria, G. E. Assessment and Validation of a Screened Coulomb Hybrid Density Functional. *J. Chem. Phys.* **2004**, *120*, 7274−7274−7.
(53) Mori-Sánchez, P.; Wu, Q.; Yang, W. Accurate Polymer Polarizabilities with Exact Exchange Density-Functional Theory. *J. Chem. Phys.* **2003**, *119*, 11001−11001−4.
(54) Champagne, B.; Pe, E. A.; Gisbergen, R. S. J. A; Baerends, E.-J.; Snijders, J. G.; Soubra-Ghaoui, C.; Robins, K. A.; Kirtman, B. Assessment of Conventional Density Functional Schemes for Computing the Polarizabilities and Hyperpolarizabilities of Conjugated Oligomers: An ab Initio Investigation of Polyacetylene Chains. *J. Chem. Phys.* **1998**, *109*, 10489−10489−10.
(55) Maroulis, G.; Haskopoulos, A.; Xenides, D. New Basis Sets For Xenon and the Interaction Polarizability of Two Xenon Atoms. *Chem. Phys. Let.* **2004**, *396*, 59−65.
(56) Maroulis, G. A Systematic Study of Basis Set, Electron Correlation, and Geometry Effects on the Electric Multipole Moments, Polarizability, and Hyperpolarizability of HCl. *J. Chem. Phys.* **1998**, *108*, 5432−5448.
(57) Maroulis, G. How Large Is the Static Electric (Hyper) Polarizability Anisotropy in HXeI? *J. Chem. Phys.* **2008**, *129*, 044314−044314−7.
(58) Cohen, H. D.; Roothaan, C. C. J. Electric Dipole Polarizability of Atoms by the Hartree−Fock Method. I. Theory for Closed-Shell Systems. *J. Chem. Phys.* **1965**, *43*, s34−s39.
(59) Buckingham, A. D. Permanent and Induced Molecular Moments and Long-Range Intermolecular Forces. *J. Adv. Chem. Phys.* **1967**, *12*, 107−142.
(60) Golberg, D.; Bando, Y.; Huang, Y.; Terao, T.; Mitome, M.; Tang, C.; Zhi, C. Boron Nitride Nanotubes and Nanosheets. *ACS Nano* **2010**, *4*, 2979−2993.
(61) Arenal, R.; Stéphan, O.; Kociak, M.; Taverna, D.; Loiseau, A.; Colliex, C. Electron Energy Loss Spectroscopy Measurement of the Optical Gaps on Individual Boron Nitride Single-Walled and Multiwalled Nanotubes. *Phys. Rev. Lett.* **2005**, *95*, 127601−127601−4.
(62) Lee, C. H.; Wang, J.; Kayashta, V. K.; Huang, J. Y.; Yap, Y. K. Effective Growth of Boron Nitride Nanotubes by Thermal Chemical Vapor Deposition. *Nanotechnology* **2008**, *19*, 455605−455605−5.
(63) Adamo, C.; Barone, V. Toward Reliable Density Functional Methods without Adjustable Parameters: The PBE0 Model. *J. Chem. Phys.* **1999**, *110*, 6158−6169.
(64) Heyd, J.; Scuseria, G. E. Efficient Hybrid Density Functional Calculations in Solids: Assessment of the Heyd−Scuseria−Ernzerhof Screened Coulomb Hybrid Functional. *J. Chem. Phys.* **2004**, *121*, 1187−1187−92.
(65) Xiao, H.; Tahir-Kheli, J.; Goddard, W. A., III. Accurate Band Gaps for Semiconductors from Density Functional Theory. *J. Phys. Chem. Lett.* **2011**, *2*, 212−217.
(66) Wan, X.; Dong, J.; Xing, D. Y. Optical Properties of Carbon Nanotubes. *Phys. Rev. B* **1998**, *58*, 6756−6756−9.
(67) Jensen, L.; Schmidt, O. H.; Mikkelsen, K. V.; Åstrand, P. O. Static and Frequency-Dependent Polarizability Tensors for Carbon Nanotubes. *J. Phys. Chem. B* **2000**, *104*, 10462−10466.
(68) Jiang, J.; Dong, J.; Wan, X.; Xing, D. Y. A New Kind of Nonlinear Optical Material: The Fullerene Tube. *J. Phys. B: At. Mol. Opt. Phys.* **1998**, *31*, 3079−3086.
(69) Jiang, J.; Dong, J.; Xing, D. Y. Size and Helical Symmetry Effects on the Nonlinear Optical Properties of Chiral Carbon Nanotubes. *Phys. Rev. B* **1999**, *59*, 9838−9841.
(70) Terauchi, M.; Tanaka, M.; Suzuki, K.; Ogino, A.; Kimura, K. Production of Zigzag-Type BN Nanotubes and BN Cones by Thermal Annealing. *Chem. Phys. Lett.* **2000**, *324*, 359−364.
(71) Okada, S.; Saito, S.; Oshiyama, A. Electronic and Geometric Structures of Multi-Walled BN Nanotubes. *Physica B* **2002**, *323*, 224−226.
(72) Brothers, E. N.; Scuseria, G. E.; Kudin, K. N. Coaxial Carbon Nanotubes as Shielded Nanowires. *J. Chem. Phys.* **2006**, *124*, 041101−041101−3.
(73) Okada, S.; Saito, S.; Oshiyama, A. Interwall Interaction and Electronic Structure of Double-Walled BN Nanotubes. *Phys. Rev. B* **2002**, *65*, 165410−165410−4.